

Comparative Investigations on Nano and Micro Titania Photocatalysts in Degradation and Mineralization: Use of Turbidity in Kinetic Studies

J. Saïen* and A.R. Soleymani

Department of Applied Chemistry, Bu-Ali Sina University, Hamedan, 65174, Iran

(Received 6 June 2008, Accepted 17 September 2008)

An attempt was made to investigate the potential of two widely used commercial nano and micro TiO₂ photocatalysts in degradation and mineralization of a typical azo dye “direct blue 71” in water. A special circulating up-flow reactor with an UV-C-150 W lamp was employed and the influence of the operational parameters was investigated. The results showed that both the photolysis and photocatalysis cause decomposition simultaneously. Despite a half concentration, the nano TiO₂ particles provide a nearly twice efficiency, and for the vital case of mineralization 98% reduction in COD after 120 min irradiation. The influence of turbidity of catalyst particles was determined with a novel method and was taken into account in kinetic studies. It was found that the bulk degradation by the OH radicals has a major role in the photocatalysis process.

Keywords: Photocatalysis, Nano and micro catalysts, Turbidity, Kinetics, Water purification

INTRODUCTION

In recent years, the advanced oxidation processes (AOP) based on the generation of very reactive oxidizing species such as hydroxyl radicals which can quickly and non-selectively oxidize a broad range of organic pollutants have been introduced as alternatives to conventional methods in water treatment [1]. Among the reported methods, the heterogeneous photocatalysis has shown to be potentially advantageous [2,3], as it can lead to qualified treatments with complete mineralization of pollutants to carbon dioxide, water and mineral acids.

Azo dyes are pollutants of high environmental impact and have been selected as the most relevant group of dyes concerning their degradation in different ways including photodegradation [4]. About 350000 tones of Azo dyes are produced worldwide annually and about 15% of this

production is released in effluents during the dyeing [3,5,6]. A number of azo dyes and their precursors have also been shown to be human carcinogens as they form toxic aromatic amines [7,8]. Due to the large degree of aromatics present in the dye molecules and the stability of modern dyes, conventional biological treatment methods are ineffective for decolorization and mineralization [9].

Titanium dioxide, as one of the most basic materials in our daily life, has emerged as an excellent photocatalyst material for environmental purification in the photocatalytic process [10]. The aim of this work was to perform a comparative study on the extensive potentials of two major type commercial titanium dioxide products, belonging to Degussa (nano particles) and Merck (micro particles) companies, in photocatalytic degradation and mineralization processes. A widely used and stable dye, called “direct blue 71 (DB71)” is chosen and the variation in concentration was considered. A suspending and circulating conic shape reactor was employed to investigate different operational parameters. For the first

*Corresponding author. E-mail: jsaien@yahoo.com

time, the known qualified effect of the turbidity of catalyst particles on the photolysis branch of UV/TiO₂ process was considered quantitatively by means of a specific manner and taken into account for the kinetic studies.

EXPERIMENTAL

All reagents were used as received without further purification. The azo dye DB71, C₄₀H₂₃N₇Na₄O₁₃S₄ (C.I. No: 34140, CAS No: 4399-55-7, MW = 1029.9) was provided from Alvan Sabet company with 99% purity (Fig. 1). Nano TiO₂ particle was a Degussa (P25) product, in the form of 80% anatase and 20% rutile with BET surface area of 50 m² g⁻¹ [11]. Mirco TiO₂ particle was a Merck (S22) product, in the form of 99% anatase with BET surface area of 14.7 m² g⁻¹ [12]. All other reagents were purchased from Merck.

Reactor Set-up and Light Source

A circulating up-flow annular and symmetric vertical photo-reactor with a conic body shape and a capacity of about one liter was employed. The details are given in our previous works [13,14]. The UV lamp was positioned centrally in the reactor, inside a quartz tube, surrounded by the substrate solution without facing any barrier. The UV lamp (66 mm length) was a 150 W mercury lamp (UV-C, medium pressure, manufactured by ARDA, French). The reactor was equipped with a water-flow jacket for regulating the temperature by means of an external circulating flow of a thermostat bath with an accuracy of ±0.1 °C. A pump, located below the reactor, provides an adjustable circulating upflow stream, receiving the solution from top of the reactor and delivering to bottom, below the lamp, promoting in this way the efficient suspension

of particles and facing the UV light. The whole reactor body was covered with reflectors of polished aluminum thin layer.

Procedure

Water solutions synthetically polluted with 50 mg l⁻¹ of dye (about 5 × 10⁻⁵ M) which is within the range of typical concentration in textile wastewaters [15,16] with a known amount of either of TiO₂ products was prepared. The pH was adjusted to the desired value by means of a pH meter (Denver, UB-10) and using dilute H₂SO₄ or NaOH solutions. The solution was then transferred to the reactor; after adjusting temperature and well mixing, the lamp was switched on to initiate the irradiation. During each experiment, circulating of suspension with a flow-rate of 5200 ml min⁻¹ was maintained to keep the suspension homogenous and to achieve uniform temperature. Samples (4 ml) were taken at different time intervals (short times at the beginning) and centrifuged, in order to separate TiO₂ particles from the samples. The operating conditions of experiments are given in Table 1.

The concentration of the dye in each sample was analyzed

Table 1. The Operational Parameter Conditions

Parameter	Value
DB71 initial concentration	50 mg l ⁻¹
TiO ₂ concentration	0-80 mg l ⁻¹
pH	4-10
Temperature	15-45 °C
Ethanol concentration	0-3% (v/v)
Irradiation time	up to 120 min

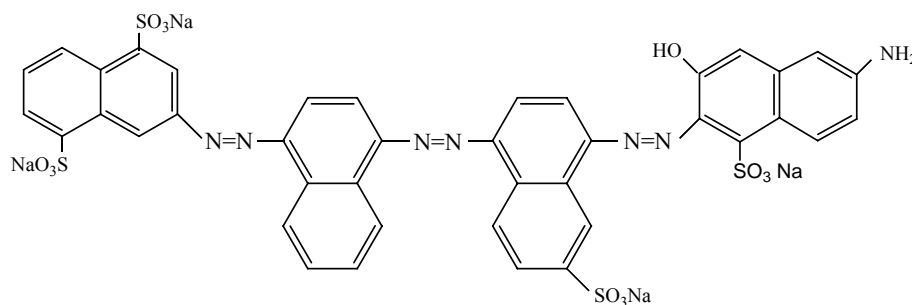


Fig. 1. The schematic of direct blue 71 (DB71) structure.

with a UV-Vis spectrophotometer (Perkin-Elmer, 55 OSE), measuring the absorbance at λ_{\max} of 584 nm and using the appropriate calibration curve [13]. It is notable that the maximum wavelength and the molar absorption coefficient of DB71 were not much dependent on the pH of solution within the range of 4-10. Using the described method, the degradation efficiency or conversion (X) of DB71 at any time can be obtained by:

$$X = \frac{C_0 - C}{C_0} \quad (1)$$

where C_0 and C are the initial and time concentrations of DB71. This conversion can be based on the appropriate amount of COD, relating to DB71 solutions. COD measurements were carried out to investigate the mineralization of the dye using the open reflux method according to the standard method procedure [17].

RESULTS AND DISCUSSION

Primary Analysis and Catalyst Influence

In a precedent study the UV-Vis absorption spectra of DB71 were investigated in the presence of either of the two TiO_2 photocatalysts, and the results are displayed in Fig. 2. The absorbance peaks at UV and visible regions are respectively attributed to the aromatic rings and azo linkages present in the structure of DB71 [18]. The bands relating to different molecular moieties of the dye are decreased with respect to time in both cases. The decrease of absorption peaks at λ_{\max} of 584 nm in Fig. 2 indicates a rapid degradation of azo dye from the -N=N-double bonds of the azo dye as the most active sites for the oxidation attack [19]. The nearly perfect disappearance of the band at 584 nm reveals that DB71 is approximately eliminated in the presence of TiO_2 suspensions after about 60 and 120 min for the nano and micro products, respectively.

The influence of catalyst concentration, within the range of 10-80 mg l^{-1} is presented in Fig. 3, for a time interval of 60 min. As it is obvious, the optimum values for nano and micro catalyst concentrations are appeared in about 20 and 40 mg l^{-1} , respectively. After these concentrations, a reduction in degradation is observed. The reason for the optimum

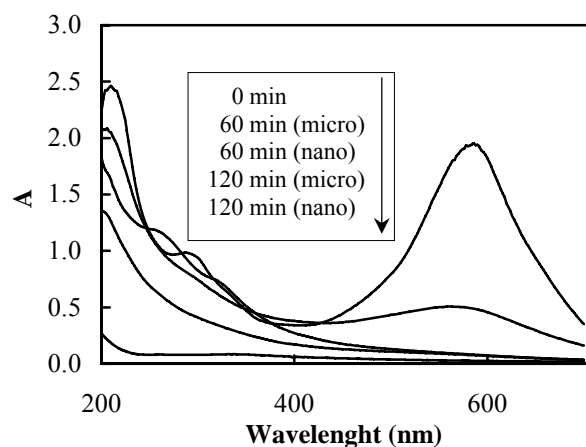


Fig. 2. The UV-Vis spectra for DB71 photocatalytic degradation, using nano and micro TiO_2 products at two typical time intervals. Conditions: $[\text{TiO}_2]_{\text{nano}} = 20 \text{ mg l}^{-1}$, $[\text{TiO}_2]_{\text{micro}} = 40 \text{ mg l}^{-1}$, natural pH 6.22 and $T = 25 \text{ }^\circ\text{C}$.

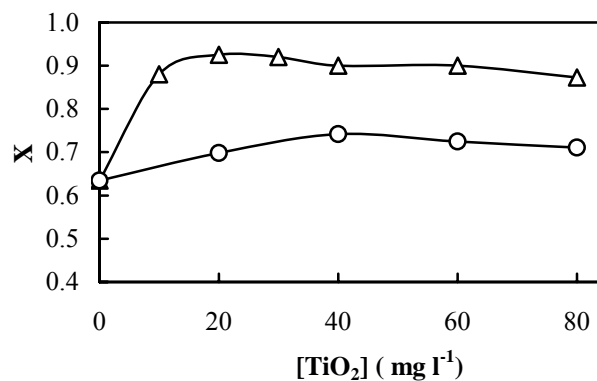


Fig. 3. Effect of catalyst concentration on degradation of DB71 after 60 min irradiation in the presence of nano (Δ) and micro TiO_2 (\circ) at natural pH and $25 \text{ }^\circ\text{C}$.

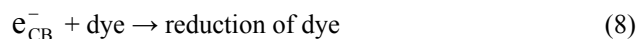
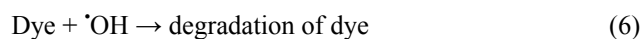
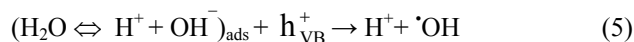
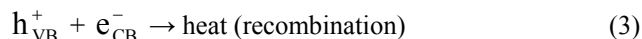
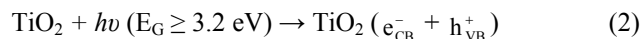
concentrations is that when enough catalyst (depending on initial substrate concentration and light intensity) is present in the suspension, and adding extra catalyst particles leads to an opacity enhancement which in turn would provide reductions in the light intensity throughout the solution [20].

The variation of degradation in the absence and presence of catalyst (with appropriate optimum concentration) was also

measured and is shown in Fig. 4. The comparison shows that the UV irradiation in the absence catalyst will result in degradation efficiencies within 63-83%, under conditions of natural pH 6.22 (with 50 mg l⁻¹ of DB71) and 25 °C, during 60 to 120 min irradiations, respectively. While, adding nano and micro catalysts caused an enhancement in degradation efficiency of about 93% in 60 min and 120 min irradiations. The results indicate that about 30% and 10% of 93% total degradation obtained during the appropriate times are due to the catalysts activity. The degradation in UV/TiO₂ process, therefore, proceeds with the simultaneous influence of photolysis and photocatalysis; however, the first one has a significantly more contribution in this regard.

The increased activity obtained with UV/TiO₂ process is due to the well known electron promotion from the valance band to the conduction band of the semi-conducting oxide to give electron-hole pairs [21,22]. The valance band hole (h_{VB}⁺) potential is positive enough to generate hydroxyl radicals from water and hydroxyl anions. Also, the conduction band electron(e_{CB}⁻) potential is negative enough to reduce the oxygen molecules present in the solution. The generated hydroxyl radicals are powerful oxidizing agents that attack organic pollutants at the surface of catalyst particles or near it (to about 500 μm) in the solution bulk [23]. Of course, the rate

of reaction of hydroxyl radicals with the substrate decreases as the distance from surface increases. The more important related equations are [4]:



The obvious advantages of the nano product, despite its lower concentration, can be discussed with the following points of view:

The smaller size provides a higher specific area of photocatalyst to be exposed to UV light which in turn leads to increase in hydroxyl radical generation.

It has been stated that the existence of rutile form accompanied with anatase form of TiO₂ will enhance the residence time of charge carriers on TiO₂ surface or retard the recombination between hole and electron (Eq. 3) that also leads to enhance in hydroxyl radical generation [24].

It is notable that there was no significant change in dye concentration when TiO₂ particles were used in darkness; *i.e.* no physical adsorption of the substrate by the catalyst particles was relevant.

Effect of pH

Figure 5 shows Effect of pH on the photocatalytic degradation of DB71 after 60 min irradiation. The interpretation of pH effects on the efficiency of dye photodegradation is a difficult task, because of its multiple roles as follows. 1) pH changes can influence the adsorption of the dye molecules onto the TiO₂ surface as an important step for direct oxidation and reduction of pollutants by h_{VB}⁺ and e_{CB}⁻ (Eqs. 7,8). For values bellow or up the pH of zero point of

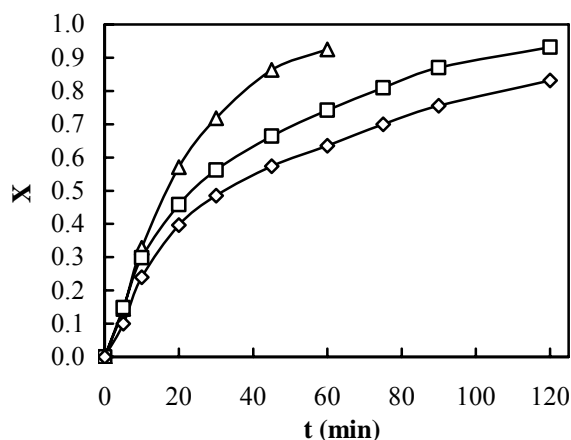


Fig. 4. Degradation-time plot for DB71 in the absence (◇) and presence of micro (□) and nano TiO₂ particles (△). Conditions: [TiO₂]_{nano} = 20 mg l⁻¹, [TiO₂]_{micro} = 40 mg l⁻¹, natural pH and T = 25 °C.

charge of 6.25 for TiO_2 , the surface is positively or negatively charged, respectively [24]; thus, the adsorption of molecules such as direct dyes can be promoted in acidic media due to their negative sulfonate groups. 2) In alkaline pH, the hydroxyl radicals are more easily generated by oxidizing more hydroxyl ions (Eq. 5) available on the TiO_2 surface and, thus, the efficiency of the process is logically increased [20,25-27].

Figure 5 shows that, for a typical time of 60 min and a pH of 6.22, the nano product provides considerably higher efficiency, while it is opposite in acidic media with pH values less than about 4.7. Regarding the fact that, in acidic media, the roll of surface active species such as h_{VB}^+ and e_{CB}^- is dominant [24], it can be concluded that under this condition the adsorption of DB71 is promoted for the micro photocatalyst. The efficiency of nano and micro products are approximately similar at pH values around 10; while the efficiency of nano product is higher at the natural pH of 6.22 with efficient generation of hydroxyl radicals. On the other hand, in the alkaline media with a pH of about 10, the generation of hydroxyl radicals from hydroxyl ions (Eq. 5) is so favored that the degradation approximately becomes independent of the type of photocatalyst and the efficiencies find the same values.

For the micro catalyst, the natural pH of 6.22 can also be considered as the optimum value, since the difference between the efficiencies at this pH and those around 4 or 10 is low and it has the advantage of no need to add any agent in order to regulate the pH of solution.

Effect of Temperature

Figure 6 presents the mild enhancing effect of temperature within the range of 15-45 °C (as the highest available temperature without considerable evaporation) on photocatalytic degradation of DB71 after 60 min irradiation. The known low activation energy of photocatalytic processes [28] can be the reason for this variation. As is demonstrated by the gradient of two lines, the increased temperature will increase the rate of photocatalytic process for the micro product to some more extent. It shows that the activation energy, belonging to the reaction in the presence of micro catalyst is higher than that for the case of nano catalyst.

Mineralization

The major importance of applied water purification

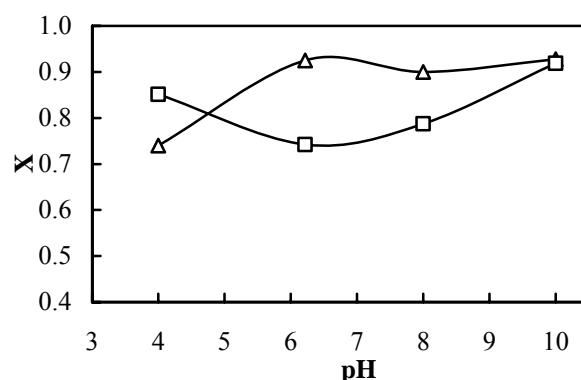


Fig. 5. Effect of pH on the photocatalytic degradation of DB71 in the presence of nano (Δ) and micro catalyst (\square), after 60 min irradiation. Conditions: $[\text{TiO}_2]_{\text{nano}} = 20 \text{ mg l}^{-1}$, $[\text{TiO}_2]_{\text{micro}} = 40 \text{ mg l}^{-1}$ and $T = 25 \text{ }^\circ\text{C}$.

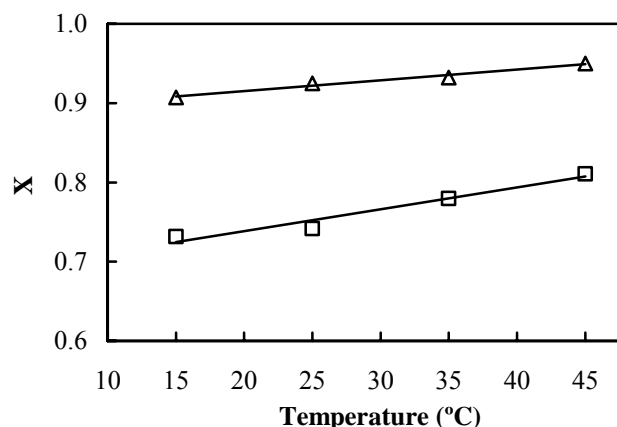


Fig. 6. Effect of temperature on photocatalytic degradation of DB71 in the presence of nano (Δ) and micro catalysts (\square), after 60 min irradiation. Conditions: $[\text{TiO}_2]_{\text{nano}} = 20 \text{ mg l}^{-1}$, $[\text{TiO}_2]_{\text{micro}} = 40 \text{ mg l}^{-1}$ and natural pH.

process is concerned on the reduction of water organic content; *i.e.* the mineralization of organic compounds. In this regard, the measurement of chemical oxygen demand (COD) is generally used for the monitoring of this case [29,30].

Figure 7 demonstrates the degradation efficiency (X) based on COD and concentration of DB71 at different times for both the nano and micro products. The results of the study of simple photolysis process are also given. The optimum

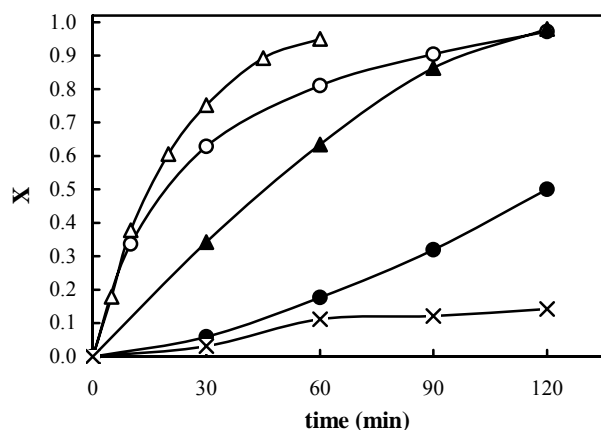


Fig. 7. Comparison between the degradation efficiencies based on solution COD and dye concentration: (Δ) nano [DB71], (\circ) micro [DB71], (\blacktriangle) nano [COD], (\bullet) micro [COD] and (\times) UV [COD]. Conditions: $[\text{TiO}_2]_{\text{nano}} = 20 \text{ mg l}^{-1}$, $[\text{TiO}_2]_{\text{micro}} = 40 \text{ mg l}^{-1}$, natural pH and $T = 45 \text{ }^\circ\text{C}$.

operating conditions were: 20 and 40 mg l^{-1} of nano and micro catalysts, natural pH and temperature of 45 $^\circ\text{C}$. The achieved efficiencies corresponding to COD removal after 120 min irradiation for mineralization with nano and micro products are 98% and 50%, respectively, while it is only 14% for the simple photolysis. It is also obvious that the nano product is much more effective in this vital case.

In general, at low levels of reactant concentration or for compounds which do not form important intermediates, complete mineralization and reactant disappearance proceed with similar efficiencies. However, at high reactant concentration levels or when stable intermediates are formed, mineralization is slower than the degradation of the parent compounds [24]. Figure 7 reveals that for DB71 which has three bi-cyclic aromatic rings in its structure, the last mentioned case is appropriate. This figure also shows that for the irradiation times longer than 120 min, the efficiency of COD removal in the case of micro photocatalyst may be increased till perfect mineralization; however, this is not the case for the photolysis. The results can prove the formation of stable compounds, resistive to photolysis process.

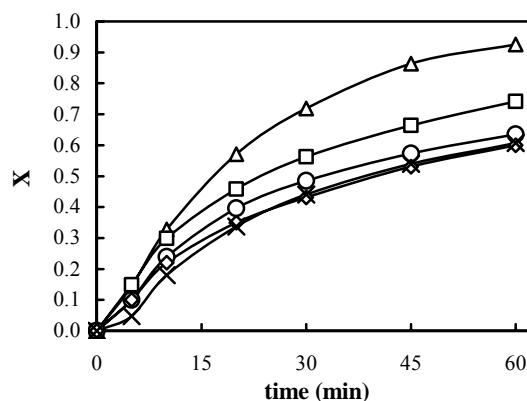


Fig. 8. Variation of degradation efficiency of DB71 vs. time for different cases: (Δ) UV/ TiO_2 (nano), (\square) UV/ TiO_2 (micro), (\circ) only UV, (\diamond) UV/ BaSO_4 (nano), (\times) UV/ BaSO_4 (micro). Conditions: $[\text{TiO}_2]_{\text{nano}} = 20 \text{ mg l}^{-1}$, $[\text{TiO}_2]_{\text{micro}} = 40 \text{ mg l}^{-1}$, natural pH and $T = 25 \text{ }^\circ\text{C}$.

Effect of Suspension Turbidity

The role of turbidity, due to the presence catalyst particles, in the reduction of degradation has already been pointed out in a qualitative manner [20]. However, for an exact evaluating of the contribution of either of the photolysis and photocatalysis branches in the UV/ TiO_2 process, a quantitative investigation is required. TiO_2 particles in suspended solutions have two different roles: 1) having a positive catalytic activity which lead to the generation of hydroxyl radicals and 2) causing turbidity in the solution which leads to unfavorable weakness of the light efficiency, compared with the case when this process is proceeding with the UV light alone. Since the light is one of the major components of the process, it is necessary to take into account the effect of suspension turbidity on the photolysis branch. To do this, we used the inert BaSO_4 particles.

A comparison was made between the solutions containing 20 mg l^{-1} of nano catalyst with turbidity of 2.290 NTU (measured with turbidimeter, HACH, 2100) and containing BaSO_4 particles with the same turbidity. Similar attempt was made for the 40 mg l^{-1} of micro TiO_2 catalyst with turbidity of 2.282 NTU. To each suspension was added 50 mg l^{-1} of the dye and the results are presented in Fig. 8. The use of BaSO_4 particles, instead of nano and micro particles, caused the UV efficiency to find an absolute reduction of about 4.3% and 4%

in photolysis, respectively. This means that the overall contribution of catalysts is actually 34.3% and 14% for the nano and micro products which were mentioned above as 30% and 10%, respectively. In this way, 12.5% and 24% errors can be avoided in calculating the percentage of contribution of nano and micro products. Neglecting the effect of turbidity can thus provide higher level of errors when higher catalyst concentrations are used.

The Role of Active Species

The contribution of oxidizing species (h_{VB}^+ , e_{CB}^- and $\cdot\text{OH}$) can be investigated using a radical scavenger [31]. As was mentioned in the above sections, the photocatalysis process can proceed in two separate routes: 1) bulk and surface degradation by hydroxyl radicals and 2) surface degradation by electron holes during the adsorption on catalyst particles. The importance of these two paths depends on the substrate structure and operational parameters such as pH. In order to evaluate these two paths, experiments with either of the catalysts were performed and different amounts of ethanol were added at natural pH. Alcohols such as ethanol are commonly used to quench hydroxyl radicals because of completely high rate constant of reaction between hydroxyl radicals and ethanol, $1.9 \times 10^9 \text{ M}^{-1} \text{ s}^{-1}$ [32]. The results are presented in Fig. 9. Adding ethanol up to 0.2% (v/v) and 0.1% (v/v) has led to a decrease of about 30% and 13% in degradation efficiency for the nano and micro products, respectively. These values represent the contribution level of hydroxyl radicals in photocatalytic degradation process for either of the catalysts. Referring to the previous section, it becomes clear that 4.3% from the total 34.3%, and only 1% from the total 14% degradation efficiency of photocatalysis process is due to direct activity of electron-hole on the surface of nano and micro TiO_2 particles, respectively.

Adding extra amounts of ethanol provides an increasing trend in the degradation efficiency for both cases. The possible formation of ethoxy radicals ($\text{C}_2\text{H}_5\text{O}\cdot$) from direct photocatalytic oxidation of ethanol and also the formation of hydroxyl radicals, produced from water, can enhance the degradation of dye molecules. It is also notable that the ethanol molecules can produce hydroxyl radicals in direct photolysis, with respect to the C-O energy bond [13]. The major role in the photocatalytic process is therefore

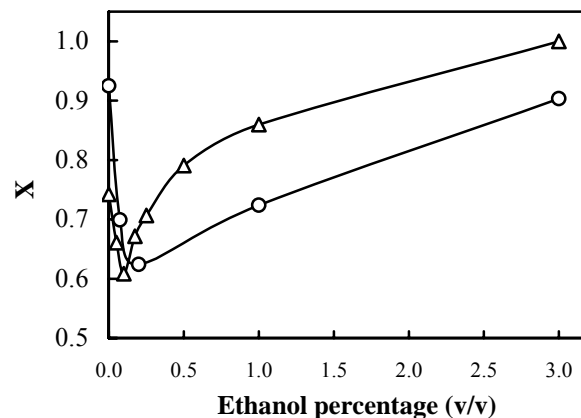


Fig. 9. Variation of degradation of DB71 vs. added ethanol after 60 min irradiation; $[\text{TiO}_2]_{\text{nano}} = 20 \text{ mg l}^{-1}$, $[\text{TiO}_2]_{\text{micro}} = 40 \text{ mg l}^{-1}$ and $T = 25 \text{ }^\circ\text{C}$: (Δ) micro, (\circ) nano.

corresponding to the hydroxyl radical species and the degradation *via* h_{VB}^+ and e_{CB}^- is negligible. Similar results have already been reported by Daneshvar *et al.* [1]. We used these results in kinetic studies.

Kinetic Studies

Due to the practical applications, the degradation kinetics of DB71 was investigated under the conditions of the appropriate optimum catalyst concentrations, natural pH and temperature of $25 \text{ }^\circ\text{C}$. From the results, it became clear that the degradation process proceeds in two parallel branches of only UV degradation and when UV is assisted with catalyst particles:

$$R = -\frac{d[\text{DB 71}]}{dt} = R_1 + R_2 \quad (9)$$

where R , R_1 and R_2 are the net degradation, the photolysis and the photocatalysis rates, respectively. The difference between the net rate and photolysis rate (considering the turbidity), obtained experimentally, can be considered as the photocatalysis branch rate.

Using the power law kinetic models in the forms:

$$R_1 = k_1[\text{DB71}]^{n_1} \quad (10)$$

$$R_2 = k_2[\text{DB71}]^{n_2} \quad (11)$$

showed a nice agreement with the experimental data for both nano and micro catalysts and also in both photolysis and photocatalysis branches of the UV/TiO₂ process. However, the use of Langmuir-Hinshelwood kinetic expression for the modeling of photocatalysis rates, which is based on the adsorption of substrate on the surface of catalyst, gives little success. This fact together with the points given in the previous section reveal that the most appropriate degradation takes place in the bulk of solution *via* OH radicals for the photocatalysis. In Eqs. (10) and (11), k_1 , k_2 , n_1 and n_2 are the appropriate rate constants and orders of reactions belonging to the photolysis and the photocatalysis branches.

Several kinetic studies in photocatalyst degradation have reported the power law models [1,33-34] and, of course, many researchers have used Langmuir-Hinshelwood model in kinetic studies [11,35,36]. In this work, to obtain the appropriate parameters of Eqs. (10) and (11), the differential method of analysis, based on the data of concentration *vs.* time, with 8 data points over 60 min for nano product and with 9 data points over 75 min for micro product, was used. Figure 10 presents the goodness of fitting of Eqs. (10) and (11) to the data. The obtained parameters are given in Table 2. The order of reactions of the photolysis and photocatalysis are more than one, indicating a rather complicated degradation mechanism. For decomposition of sodium dodecylbenzene sulfonate solution, for instance, an order of 1.32 [33], for degradation of Auramine O a second order [34] and for degradation of azo dye acid red 14 a first order [1] kinetic model have already been reported. This later order in addition to its rate constant values, reported for the degradation of acid red 14, are very close to the values found in this work for the photocatalysis with the nano particles.

Based on the above discussions and to have a convenient scheme of the obtained results, corresponding to the

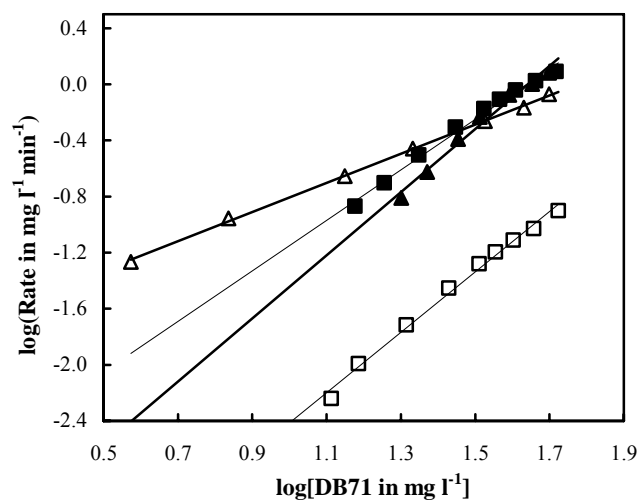


Fig. 10. The variation of DB71 degradation rates *vs.* its concentration for the photolysis and photocatalysis processes: (Δ) photocatalysis (nano), (■) photolysis (micro), (▲) photolysis (nano) and (□) Photocatalysis (micro). Conditions: [TiO₂]_{nano} = 20 mg l⁻¹, [TiO₂]_{micro} = 40 mg l⁻¹, natural pH and T = 25 °C.

contribution level of different parameters and species in the degradation process, Fig. 11 can be useful as a global and summarized schematic presentation.

CONCLUSIONS

The present investigation illustrates the following conclusions: (i) between the two utilized types of TiO₂ photocatalyst, Degussa product with nano particles provided significantly higher efficiency in degradation and mineralization of azo dye direct blue 71 with an industrial

Table 2. Kinetic Parameters of DB71 Degradation

Catalyst	n_1	k_1	n_2	k_2
Nano	2.25	2.02×10^{-4} (mg l ⁻¹) ^{-1.25} min ⁻¹	1.04	1.42×10^{-2} (mg l ⁻¹) ^{-0.04} min ⁻¹
Micro	1.83	9.92×10^{-4} (mg l ⁻¹) ^{-0.83} min ⁻¹	2.16	2.58×10^{-5} (mg l ⁻¹) ^{-1.16} min ⁻¹

Comparative Investigations on Nano and Micro Titania Photocatalysts

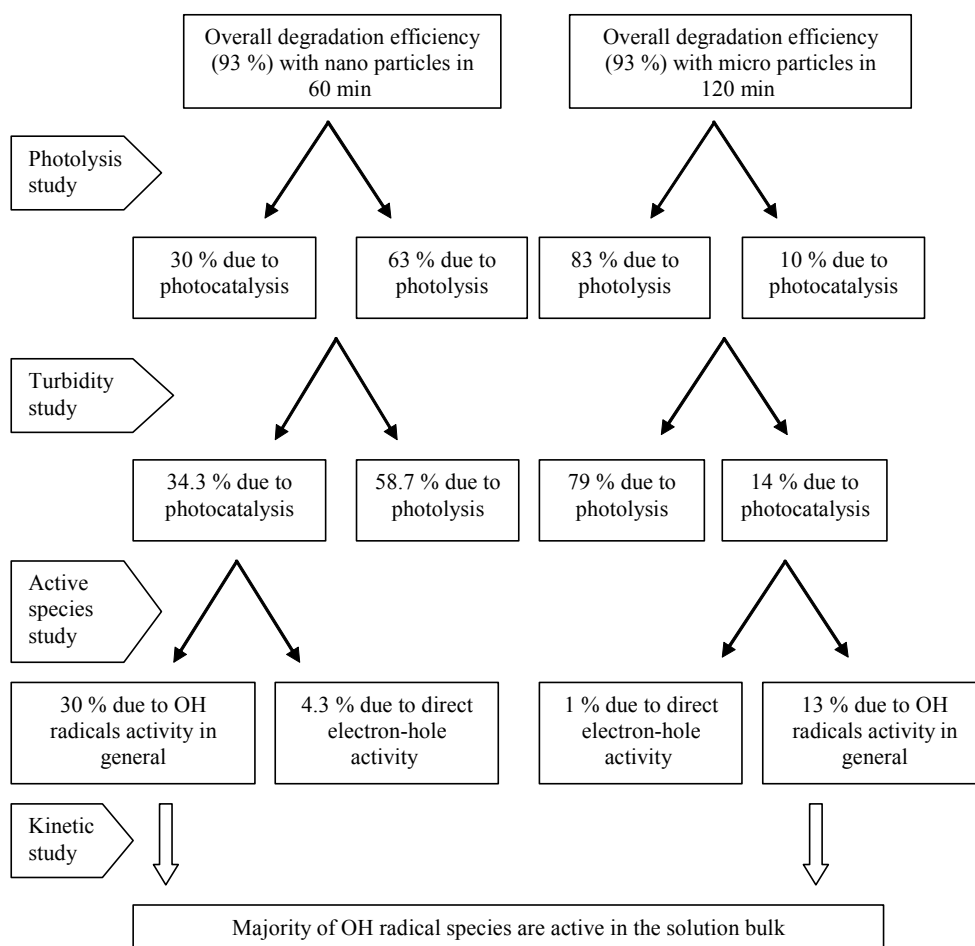


Fig. 11. A schematic presentation of the results corresponding to the degradation process.

representation concentration of 50 mg l^{-1} under optimum conditions, (ii) the moderate and the most suitable conditions for degradation and mineralization of DB71 found to be: catalyst concentrations: 40 mg l^{-1} (micro) and 20 mg l^{-1} (nano), pH: 6.22 (natural) and temperature: $45 \text{ }^{\circ}\text{C}$, (iii) COD investigations revealed the importance of using photocatalysts where a nearly perfect mineralization of the dye can be obtained with the nano catalyst and about 50% with micro particles in 120 min under the optimum conditions; it is while only about 14% can be obtained with photolysis in the same time, (iv) it was found that, in acidic media, the degradation of the dye is promoted only with the micro product; while in the alkaline media, the efficiency of degradation obtained with either of the catalysts tends to reach the same values, (v) the

efficiency of degradation is not much affected by temperature; however, in the case of micro product the effect is higher, (vi) considering the catalyst particles turbidity, significant levels of error can be prevented in calculations of catalysts contribution, (vii) it became clear that the bulk degradation by hydroxyl radicals has the major role in the photocatalytic process compared with the surface degradation and (viii) the power law kinetic model showed a nice agreement with experimental data for both utilized catalysts in the photocatalytic degradation process.

ACKNOWLEDGEMENTS

The authors wish to remember of blessed memory of late

Professor Nezamodin Daneshvar at the Faculty of Chemistry, University of Tabriz, for the assistance in providing the nano photocatalyst.

REFERENCES

- [1] N. Daneshvar, D. Salari, A.R. Khataee, J. Photochem. Photobiol. A: Chem. 157 (2003) 111.
- [2] A. Hoaus, H. Lachheb, M. Ksibi, E. Elaloui, C. Guillard, J.M. Hermann, Appl. Catal. B: Environ. 31 (2001) 145.
- [3] A. Fujishima, K. Hashimoto, T. Watanabe, *TiO₂ Photocatalysis, Fundamentals and Applications*, Bkc: Tokyo, 1999.
- [4] I.K. Konstantinou, T.A. Albanis, Appl. Catal. B: Environ. 49 (2004) 1.
- [5] N.M. Mahmoodi, M. Arami, N.Y. Limaee, N.S. Tabrizi, Chem. Eng. J. 112 (2005) 191.
- [6] C. Bauer, P. Jecque, A. Kalt, J. Photochem. Photobiol. A: Chem. 140 (2001) 87.
- [7] M. Styliidi, D.I. Kondarides, X.E. Verykios, Appl. Catal. B: Environ. 40 (2003) 271.
- [8] C. Gomes da Silva, J.L. Faria, J. Photochem. Photobiol. A: Chem. 155 (2003) 133.
- [9] N. Daneshvar, M. Rabbani, N. Modirshahla, M.A. Behnajady, Chemosphere 56 (2004) 895.
- [10] A. Fujishima, X. Zhang, Comptes Rendus Chimie 9 (2006) 750.
- [11] N. Daneshvar, M. Rabbani, N. Modirshahla, M.A. Behnajady, J. Photochem. Photobiol. A: Chem. 168 (2004) 39.
- [12] C. Karunakaran, S. Senthilvelan, S. Karuthapandian, K. Balaraman, Catal. Commun. 5 (2004) 283.
- [13] J. Saien, A.R. Soleymani, J. Hazard. Mater. 144 (2007) 506.
- [14] J. Saien, H. Nejati, J. Hazard. Mater. 148 (2007) 491.
- [15] N. Daneshvar, A. Aleboyeh, A.R. Khataee, Chemosphere 59 (2005) 761.
- [16] N.M. Mahmoodi, M. Arami, N.Y. Limaee, N.S. Tabrizi, Chem. Eng. J. 112 (2005) 191.
- [17] APHA Standard Methods for Examination of Water and Wastewaters, 17th ed., American Public Health Association, Washington DC, 1989.
- [18] W. Feng, D. Nansheng, H. Helin, Chemosphere 41 (2000) 1233.
- [19] Z. Sun, Y. Chen, Q. Ke, Y. Yang, J. Yuan, J. Photochem. Photobiol. A: Chem. 149 (2002) 169.
- [20] M.S.T. Goncalves, A.M.F. Oliveira-Campos, E.M.M.S. Pinto, P.M.S. Plasencia, M.J.R.P. Queiroz, Chemosphere 39 (1999) 781.
- [21] R.I. Bickley, M.J. Slater, W.J. Wang, Process Safety & Environ. Protect. 83 (2005) 205.
- [22] W.J. Masschelein, in: R.G. Rice (Ed.), *Ultraviolet Light in Water and Wastewater Sanitation*, Lewis Publishers, Boca Raton, 2002.
- [23] A. Fujishima, T.N. Rao, D.A. Tryk, J. Photochem. Photobiol. C: Photochem. Reviews 1 (2000) 1.
- [24] M.R. Hoffmann, S.T. Martin, W. Choi, D.W. Bahnemann, Chem. Rev. 95 (1995) 69.
- [25] Z. Shourong, H. Qingguo, Z. Jun, W. Bingkun, J. Photochem. Photobiol. A: Chem. 108 (1997) 235.
- [26] C. Galindo, P. Jacques, A. Kalt, J. Photochem. Photobiol. A: Chem. 130 (2000) 35.
- [27] S. Sakthivel, B. Neppolian, M. Palanichamy, B. Arabindoo, V. Murugesan, Indian J. Chem. Tech. 6 (1999) 161.
- [28] R. Terzian, N. Serpone, J. Photochem. Photobiol. A: Chem. 89 (1995) 163.
- [29] B. Neppolian, H.C. Choi, S. Sakthivel, B. Arabindoo, V. Murugesan, Chemosphere 46 (2002) 1173.
- [30] F. Zhang, J. Zhao, T. Shen, H. Hidaka, E. Pelizzetti, N. Serpone, Appl. Catal. B: Environ. 15 (1998) 147.
- [31] G. Al-Sayyed, J.C.D. Oliveira, P. Pichat, J. Photochem. Photobiol. A: Chem. 58 (1991) 99.
- [32] A.A. Khodja, T. Sehili, J.F. Pilichowski, P. Boule, J. Photochem. Photobiol. A: Chem. 141 (2001) 231.
- [33] J. Saien, R.R. Ardjmand, H. Iloukhani, Phys. Chem. Liq. 41 (2003) 519.
- [34] K. Vasanth Kumar, K. Porkodi, A. Selvaganapathi, Dyes and Pigments 75 (2007) 246.
- [35] M.H. Priya, G. Madras, Ind. Eng. Chem. Res. 45 (2006) 482.
- [36] Y. meng, X. Huang, Y. Wu, X. Wang, Y. Qian, Environ. Pollut. 117 (2002) 307.